© 1977 by: Schweizerische Chemische Gesellschaft, Basel,
Société suisse de chimie, Bâle - Società svizzera di chimica, Basilea
ISSN 0018-019X
Nachdruck verboten - Tous droits réservés - Printed by Birkhäuser AG, Basel, Switzerland
Erscheint 9mal jährlich - Paraît 9 fois par an

180. MO-Calculation of the Optical Activity of Oligopeptides. I. Computational Procedure and Application to Small Helices

by **Georges Wagnière, Max Iseli, Rudolf Geiger**[1]) and **Werner Gans**[2])

Institute of Physical Chemistry, University of Zürich, Rämistr. 76, CH-8001 Zürich

(26.V.77)

Summary

All-valence electron calculations on the chiroptic properties of oligopeptides rapidly become intractable, as the size of the molecule increases. A *Frozen Core* procedure is here proposed, which is inspired by the PPP method. It takes explicitly into account only the (pseudo) π electrons and oxygen n electrons of the amide moieties, as well as the π electrons of eventual long-wavelength absorbing side-groups. Local n-π interaction is taken into account by an adjustable parameter. Other parameters are calibrated on the isolated amide and carbonyl chromophores. The method then follows the usual SCF-CI procedure. Rotatory strengths and f-values for the transitions are computed without further approximations, as previously described. Comparisons with results from exciton calculations and experimental data on polypeptides show the computed quantities to have a consistent and satisfactory order of magnitude.

1. General introduction. - Twenty years ago *Moffitt* [1] [3] and *Fitts & Kirkwood* [2] [3] computed by the exciton model the optical activity of the π-π^* bands of α-helical polypeptides. *Moffitt,* using periodic boundary conditions, arrived at definite selection rules and clearcut predictions: If one considers the electric dipole-electric dipole interaction (μ_i-μ_j mechanism) of the individual long-wavelength π-π^* transitions ($\lambda \sim 190$ nm) in each amide chromophore, the composite system, *i.e.* the helix, shows two transitions: One transition at longer wavelength ($\lambda \sim 210$ nm) polarized parallel to the axis of the helix, another degenerate one at shorter wavelength ($\lambda \sim 190$ nm) polarized perpendicularly. In the righthanded helix the rotatory strength of the former is negative, that of the latter positive (see *Fig. 1*). It was then shown that *Moffitt*'s approach contained an inconsistency [3]: namely, that of assuming periodic boundary conditions - suited for quasi-infinite helices -, while at the same time using the nonretarded spatially averaged expression for the rotatory strength applicable to randomly oriented molecules of much smaller size than the wavelength of light. Later investigations have dealt with this question in detail [4-6]. *Moffitt*'s original predictions, however, appeared to agree essentially

[1]) Present address: Physical Laboratory, *Hoffmann-La-Roche,* Ltd., Basel.
[2]) Present address: Institute of Physical Chemistry, ETH, Zürich.

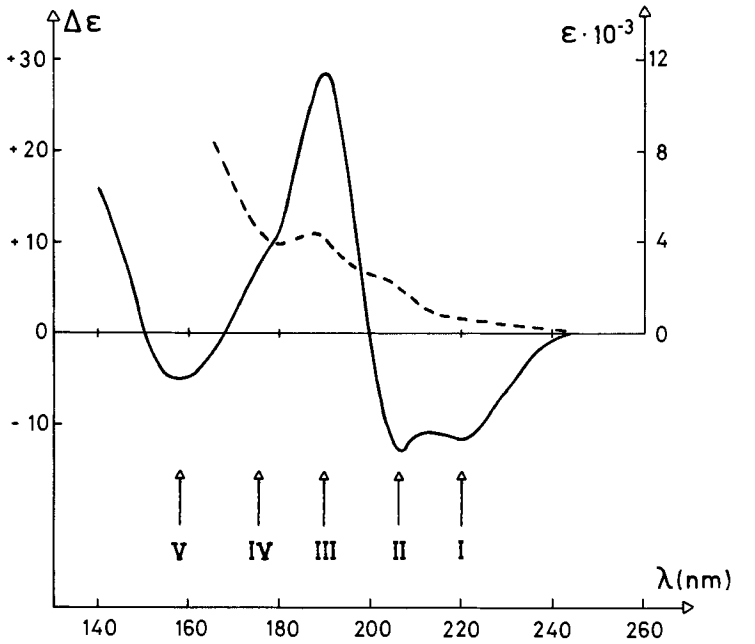

Fig. 1. *CD and absorption spectrum of poly-γ-methyl glutamate in hexafluoro-2-propanol,* as measured by *Johnson & Tinoco* and redrawn from [25]. The generally accepted assignment is: I(n-π^*) band, II(π-π^*) parallel band, III(π-π^*) perpendicular band. The shoulder IV at 175 nm is considered by *Johnson & Tinoco* to arise from a n→σ transition. The negative *Cotton* effect V might conceivably be connected to higher π-π^* transitions

with experiment and lead to a first quantitative basis for the interpretation of ORD curves of helical proteins [7].

By the refinement of experimental techniques, in particular the possibility of easily measuring CD, the existence of a negative n-π^* band in α-helical polypeptides was subsequently discovered in the 210–240 nm region, in front of the π-π^* band [8–12]. It was initially concluded that the optical activity of this n-π^* band arises largely by a local n-π mixing mechanism (μ_i-m_i mechanism), due to the asymmetric environment of each individual amide chromophore [13]. Attempts have since been made to find a unified description of both the π-π^* and n-π^* *Cotton* effects in peptides, – essentially by a more general formulation of the exciton model [14–16]. In it the interaction of n-π^* states with π-π^* states enters as electric quadrupole-electric dipole interaction (μ_i-m_j mechanism). On the other hand, the question can be raised if a semiempirical molecular orbital approach would not be suited just as well to tackle such a problem. Yet in quasi-infinite systems, full exploitation of periodic (cyclic) boundary conditions to simplify SCF and CI equations [17] does not suffice to make the problem tractable.

Within the last decade there has been a surge of interest in the chemical and physical properties of small linear and cyclic peptides with up to ten or twelve amino acid units. It has also been found that peptides of small size may exist in α-helical form [18], showing that the occurrence of this type of conformation is not

restricted to very large polypeptides. Yet molecules of even such limited size contain already several hundred valence electrons, and the applicability of current all-valence procedures such as the CNDO method to compute excited states, electric and magnetic transition moments remains questionable. The aim of the present investigation is, therefore, to assess the limits of such an all-valence electron approach and to suggest an even simpler procedure, especially adapted to describe the lowest excited states in oligopeptides, both n-π^* and π-π^*, and being able to take into account the additional interaction with eventual long-wavelength-absorbing side-chains. This computational procedure is not meant as a substitute for the exciton model, but rather as a complement to it.

2. Preliminary all-valence calculations. – A series of exploratory *Extended Hückel* calculations [19] with standard parametrization [20] on (hypothetical) α-helical di-, tri- and penta-L-alanine do not give a reasonable energetic sequence for the filled valence orbitals. The relative energy of quite typically localized oxygen nonbonding orbitals is too low, that of more delocalized σ orbitals is too high. The method must fail for even the roughest spectroscopic predictions.

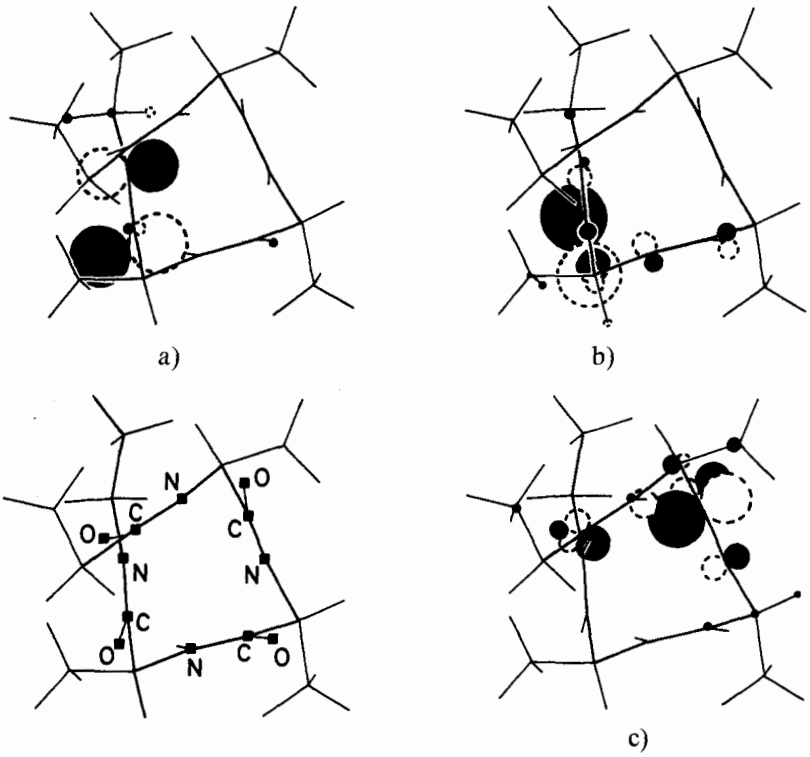

Fig. 2. *Computer plots* [23] *of selected higher canonical CNDO/SCF orbitals of tetra*-L-*alanine* (polar end groups replaced by appropriate nonpolar fragments): a) Orbital 62, predominantly localized on the first amide group, of π-type. b) Orbital 63 (highest filled orbital; the molecule considered has 126 valence electrons), predominantly localized on the first amide group, of oxygen-n-type. c) Orbital 64, predominantly localized on the third amide group, of π^*-type

A clearer picture emerges from CNDO calculations [21] [22] on such molecules. In spite of the ZDO approximation, electron interaction effects make local symmetry properties come out correctly already at the SCF level. *Figures 2a, b, c* show graphical representations [23] of the two highest occupied and one of the lowest unoccupied canonical SCF/CNDO orbitals of tetra-L-alanine in a righthanded α-helical conformation. These orbitals may be identified as of n-, π- and π^*-type, respectively. It is of interest that the n and π orbitals occur in the same energy region. The extent of localization of these canonical orbitals on particular amide groups is also striking.

The transition energies and rotatory strengths of α-helical tetra-L-alanine computed by the CNDO/SCF-CI method agree at best only qualitatively with spectroscopic data on polypeptides (see *Table 1* and *Fig. 1*), and an extension of such computations to larger systems does not seem promising, however.

Table 1. *Transition wavelengths, components of the electric* (in au) *and magnetic transition moments, rotatory strengths of tetra-L-alanine in righthanded α-helical conformation, computed by the CNDO/SCF-CI method.* The polar end groups were replaced by appropriate nonpolar fragments. Note the relatively weak negative (n-π^*) band consisting of transitions 1–4. The CNDO parametrization is described in [21] [22] [33] and references listed therein. The z-axis coincides with the helix axis

Excited state b	λ (nm)	$\langle\vec{\nabla}\rangle_x$	$\langle\vec{\nabla}\rangle_y$	$\langle\vec{\nabla}\rangle_z$	$\langle\vec{r}\times\vec{\nabla}\rangle_x$	$\langle\vec{r}\times\vec{\nabla}\rangle_y$	$\langle\vec{r}\times\vec{\nabla}\rangle_z$	$R_{ab}\cdot 10^{40}$ (cgs)	Type
1	269	−0.04537	−0.01944	−0.01342	0.0991	−0.7300	0.6901	0.6	
2	267	−0.00272	0.04919	−0.0099	−0.5413	0.0828	0.7335	−2.4	$n\pi^*$
3	259	0.04965	−0.00258	−0.01555	0.1502	0.3121	0.7098	−5.9	
4	257	0.02596	−0.03538	−0.02135	0.7753	0.2861	0.7239	−7.3	
5	183	0.10470	−0.05766	0.04249	1.2699	0.3755	−0.0864	102.1	
6	178	0.14919	0.19195	0.24222	−0.8327	2.2191	−0.5173	162.4	$\pi\pi^*$
7	174	−0.10183	−0.05181	0.30337	0.6074	−0.9676	−0.7198	−207.4	
8	168	0.14375	−0.12781	0.06646	1.1495	1.5511	−0.2024	− 40.4	

3. The *Frozen Core* (FC) approach. - We start from the idea that local σ-π separation is approximately valid for the individual amide groups. Deviations from this local planar symmetry, due to the asymmetry of the molecule as a whole, is to be expressed by a local parameter Λ_i for each amide monomer i. The AO basis consists solely of the (pseudo) $2p_\pi$ orbitals of the atoms belonging to the amide groups, of the $2p_n$ orbitals of the oxygen atoms of the amide groups and of the (pseudo) $2p_\pi$ orbitals of atoms belonging to eventual unsaturated, long-wavelength absorbing side groups. Each amide group is thus viewed as a 6 electron system (4 π electrons, 2 nonbonding electrons; see *Fig. 3*). This approach is very similar to the PPP method [26] with the additional inclusion of nonbonding electrons.

If n designates the $2p_{nO}$ and O the $2p_{\pi O}$ (oxygen) orbital of a given amide group in the polymer, then the matrix elements of the *Fock* operator between these orbitals are, in usual notation [21] [26] [27]:

$$F_{nn} = h_{nn} + \sum_s P_{ss}\,\gamma_{ns} - \frac{1}{2} P_{nn}\,\gamma_{nn} \qquad (1a)$$

where $$h_{nn} = -I'_n - \sum_{s \neq n} z_s \gamma_{ns}, \tag{1b}$$

and $$F^{(i)}_{nO} = \Lambda_i - \frac{1}{2} P_{nO} \gamma_{nO} \tag{1c}$$

The index s goes over all orbitals in the polymer which enter the calculation. The parameter Λ couples the $2p_{nO}$ and $2p_{\pi O}$ orbital in the given amide group. Λ may take on different values for different amide groups. Core matrix elements between the nonbonding oxygen orbital n and the $2p_\pi$ orbitals of the atoms C and N within the same amide group are, for simplicity, set equal to zero (see *Table 3a*).

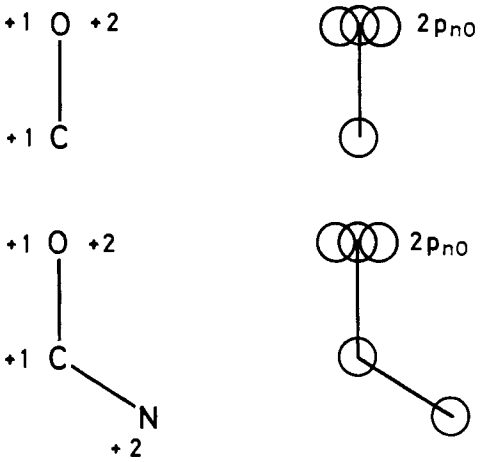

Fig. 3. *Core charges and basis orbitals entering the* Frozen Core Calculation *for the carbonyl and amide group*

Core matrix elements between different monomers are neglected in a first approximation. Nondiagonal *Fock* matrix elements between orbitals on different amide groups therefore vanish. However, all electron repulsion integrals γ between all relevant atomic orbitals in the polymer enter the calculation in the frame of the ZDO approximation.

The parameters are calibrated on the electronic properties of the isolated amide group and carbonyl group (see *Table 2*) [28–30]. At the same time, care is taken to stay as close as possible to current PPP parametrization [31] [32]. Critical quantities for the amide group are the effective valence state ionization potential for the nonbonding oxygen electrons I'_n and the electron repulsion integrals $\gamma_{nn} \equiv \langle nn|nn\rangle$, $\gamma_{nO} \equiv \langle nO|nO\rangle$ and $\gamma_{nC} \equiv \langle nC|nC\rangle$ ($C \equiv 2p_{\pi C}$). In the calculations reported here we have adopted $I'_n = 26.80$ eV; $\gamma_{nn} = 14.50$ eV, $\gamma_{nO} = 10.14$ eV, $\gamma_{nC} = 7.91$ eV (see *Table 3b*). The above γ values are perhaps unrealistically small. It is, however, not entirely trivial to reproduce the experimental data listed in *Table 2*, be it in an approximate, yet equilibrated manner.

Table 2. *Experimental ionization energies* [28] *and transition wavelengths* [29] [30] for the *isolated carbonyl* (formaldehyde) *and amide* (formamide) *group, compared with SCF orbital energies* ε *and transition wavelengths computed by the FC method using the parameters listed in* Tables 3a, b

	Experimental [28–30]		Computed	
Carbonyl group	I(π)	14.1–14.4 eV	ε_π	14.16 eV
	I(n)	10.9 eV	ε_n	11.65 eV
	nπ^*	300 nm	nπ^*	302 nm
	$\pi\pi^*$	160 nm	$\pi\pi^*$	141 nm
Amide group	I(π)	10.5 eV	ε_π	9.83 eV
	I(n)	10.1 eV	ε_n	10.51 eV
	nπ^*	220 nm	nπ^*	238 nm
	$\pi\pi^*_\Sigma$	170–190 nm	$\pi\pi^*_\Sigma$	176 nm
	$\pi\pi^*_\uparrow$	145–160 nm	$\pi\pi^*_\uparrow$	120 nm

Table 3a. *Core matrix elements in eV for the amide chromophore in the* Frozen Core *calculations.* $N \equiv 2p_{\pi N}$, *etc.* $n \equiv 2p_{nO}$

	N	C	O	n
N	−20.90			
C	− 3.15	−10.45		
O	0.	− 3.30	−15.65	
n	0.	0.	Λ	−26.80

Table 3b. *Electron repulsion integrals in eV for the amide chromophore*

	N	C	O	n
N	12.27			
C	7.65	10.53		
O	5.91	8.42	14.50	
n	5.91	7.91	10.14	14.50

In order to reproduce the n-π^* band, the n-π mixing parameter Λ is of key importance. The n-π mixing at the SCF level allows the various local nπ^* excitations to couple to the $\pi\pi^*$ excitations through configuration interaction and to borrow contributions to the electric dipole transition moment from them. For $\Lambda = 0$, the nπ^* and $\pi\pi^*$ configurations do not mix.

4. Computational steps. – We are now able to summarize the course of a calculation, as programmed for our purposes: The input consists of:

1) The coordinates of the atoms belonging to the amide groups. These are obtained either from crystallographic data or from calculations of minimum energy conformations. If the molecule contains sidechains contributing to the long-wavelength electronic spectrum, such as the phenyl group in phenyl alanine, or the indole moiety in tryptophane, these are included in the calculation and treated as additional monomeric chromophore(s);

2) The core matrix, including the parameter Λ_i for every amide group i;

3) The matrix of electron repulsion integrals – or γ matrix – is either read in completely or computed in parts automatically from 1) by the charged sphere (or by other) approximation.

The transition energies and wavefunctions are calculated by the standard SCF and single-excitation CI procedure. All $n\pi^*$ and $\pi_2\pi^*$ (or, in another customary notation, $\pi^0\pi^-$) configurations are taken into account.

From the approximate wavefunctions the electric dipole transition moments and the magnetic dipole transition moments are computed without further approximations, taking into account all one- and multi-center terms [34]. The axis of the $2p_\pi$ function on a given atom in a given monomeric chromophore (amide group, phenyl group, *etc.*) is assumed to be perpendicular to the plane of that particular chromophore [32]. The axis of a given oxygen nonbonding orbital $2p_{nO}$ in an amide group is assumed to lie in the plane of the chromophore and to be perpendicular to the C–O axis. These different p orbitals enter the calculation of the transition moments as *Slater* functions with standard exponents (C 1.625, N 1.950, O 2.275) and must then be expressed in terms of their components in the molecular frame of reference. To ensure the origin-independence of the rotatory strength, the electric dipole transition moments are computed in the dipole velocity form.

For a given transition $a \rightarrow b$ the rotatory strength is then obtained from the formula [33]

$$R_{ab} = \frac{e^2\hbar^3}{m^2c(E_b - E_a)} \sum_{ik} \sum_{i'k'} B_{ik} B_{i'k'} \langle \varphi_i | \vec{\nabla} | \varphi_k \rangle \langle \varphi_{i'} | \vec{r} \times \vec{\nabla} | \varphi_{k'} \rangle \qquad (2)$$

in which φ_i, φ_k are appropriate SCF MO's and B_{ik} designate single-excitation CI coefficients.

5. Results and discussion. – The results shown in *Fig. 4* serve to calibrate the n-π-mixing parameter Λ. For simplicity we adopt here the same value of Λ_i for each amide group i, disregarding end-effects. A positive value of Λ leads to the correct negative sign for the n-π^* CD band in the righthanded α-helix. If the absolute value of Λ rises beyond a certain limit of about 1.0 eV, however, the long-wavelength part of the n-π^* band changes sign.

In *Fig. 5* the rotatory strengths of righthanded α-helical tri-, hexa- and nonaglycine, computed with $\Lambda = 0.5$ eV, are compared with each other (see also *Table 4*). We designate the transitions appearing in the region 230–250 nm

Table 4. Results of a Frozen Core *calculation on righthanded α-helical tetra-glycine.* Compare with *Table 1* and note the stronger negative $n\pi^*$ band. The adopted value of Λ for all monomers is 0.5 eV. The z-axis coincides with the helix axis. In the CI calculation the higher $\pi_1\pi^*$ ($\pi^+\pi^-$) configurations are also included

Excited state b	λ (nm)	$\langle\vec{\nabla}\rangle_x$	$\langle\vec{\nabla}\rangle_y$	$\langle\vec{\nabla}\rangle_z$	$\langle\vec{r}\times\vec{\nabla}\rangle_x$	$\langle\vec{r}\times\vec{\nabla}\rangle_y$	$\langle\vec{r}\times\vec{\nabla}\rangle_z$	$R_{ab} \cdot 10^{40}$ (cgs)	Type
1	257	−0.01957	−0.01698	−0.01383	0.1301	−0.0674	0.3123	− 7.6	$n\pi^*$
2	254	0.01601	−0.01471	−0.03073	0.0460	0.2279	0.6483	− 29.6	
3	239	−0.02020	0.03094	−0.04515	−0.0462	−0.0565	0.5743	− 33.1	
4	233	−0.00546	0.02868	−0.04095	−0.3859	−0.0634	0.4821	− 23.4	
5	187	−0.07243	−0.09304	0.03371	−0.3184	−1.1202	−0.0620	121.3	$\pi\pi^*$
6	182	0.16941	−0.20885	0.22536	1.8908	−0.1789	−0.4869	232.8	
7	171	−0.05404	0.14065	0.30375	−0.7677	−0.3406	−0.7231	−199.9	
8	167	0.20299	0.13182	−0.04040	−0.9176	1.0255	0.1450	− 49.0	

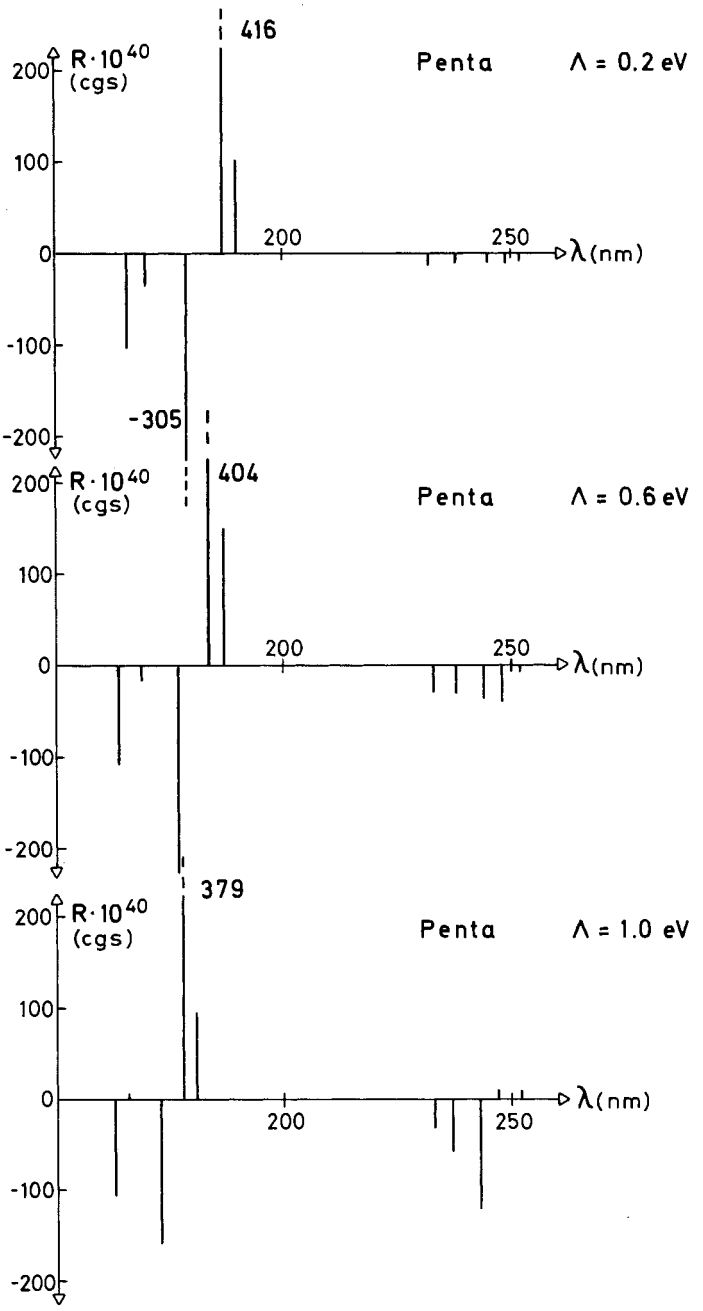

Fig. 4. *Transition energies and rotatory strengths in righthanded α-helical pentaglycine, computed by the FC procedure, for different values of the local n-π coupling parameter Λ.* Note that for $\Lambda = 1.0$ eV the longest-wavelength transitions of n-π^*-type near 250 nm change sign

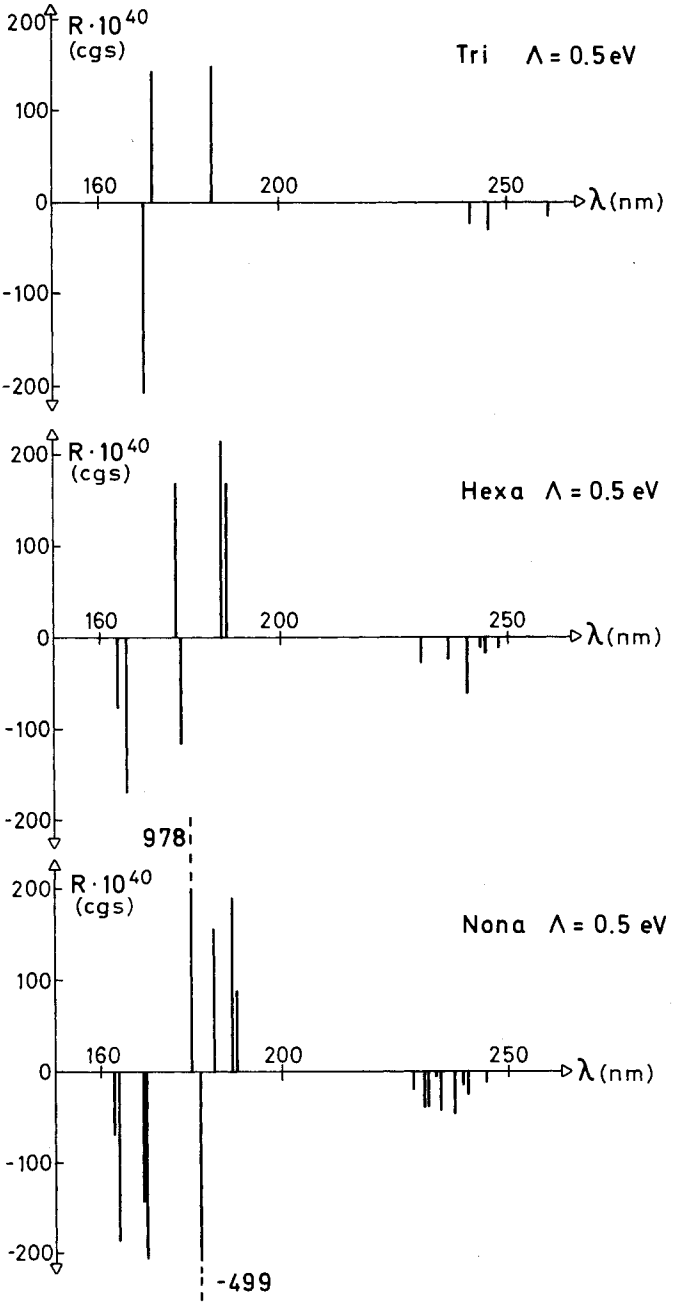

Fig. 5. *Transition energies and rotatory strengths in righthanded α-helical tri-, hexa- and nonaglycine, computed by the FC procedure, for Λ = 0.5 eV*

collectively as (n-π^*), those below 200 nm, according to the sign of the rotatory strength, collectively as $(\pi\text{-}\pi^*)_+$ and $(\pi\text{-}\pi^*)_-$ respectively. If within a computed composite band we add the rotatory strengths and divide by the number of monomers, we find for nonaglycine in cgs units:

$$R(\text{n-}\pi^*) = -27 \cdot 10^{-40} \qquad R(\pi\text{-}\pi^*)_+ = 157 \cdot 10^{-40} \qquad R(\pi\text{-}\pi^*)_- = -122 \cdot 10^{-40}.$$

Making use of the approximate formula

$$R \approx 23 \cdot 10^{-40} \sqrt{\pi}\, \frac{\Delta}{\lambda_0} \Delta\varepsilon_{max} \tag{3}$$

and assuming $\Delta/\lambda_0 = 0.06$ for the composite (n-π^*) band, and 0.09 for the two (π-π^*) bands separately, one obtains the predicted values

$$\Delta\varepsilon_{max}(\text{n-}\pi^*) = -11.0 \qquad \Delta\varepsilon_{max}(\pi\text{-}\pi^*)_+ = +42.8 \qquad \Delta\varepsilon_{max}(\pi\text{-}\pi^*)_- = -33.2$$

which agree with experiment as to order of magnitude (see *Fig. 1*). In their calculations on small polymers *Madison & Schellman* [16] assume bandwidths of 12 nm and 14 nm for the (n-π^*) and (π-π^*) bands respectively. Our numbers correspond to bandwidths of about 14 nm and 17 nm for the composite bands. Another procedure consists in attributing a *Gauss* curve to every single predicted transition and to compute the spectrum as superposition of these curves. This is shown in *Fig. 6* for nonaglycine. The result also depends sensitively on the chosen bandwidth.

Concerning the energetic sequence of the $(\pi\text{-}\pi^*)_+$ and $(\pi\text{-}\pi^*)_-$ bands, there appears to be a discrepancy between our results on oligopeptides on one hand, and the spectra of polymers and the predictions by *Moffitt* on the other. In the quasi-infinite righthanded α-helix the $(\pi\text{-}\pi^*)_-$ band is the 'parallel' band and

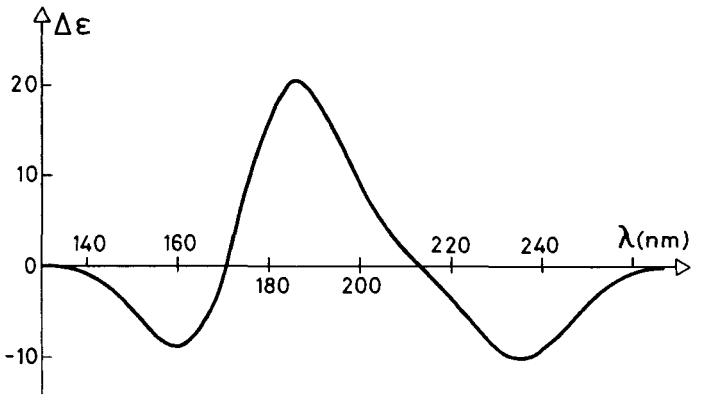

Fig. 6. *Computed CD spectrum for righthanded α-helical nonaglycine, based on the rotatory strengths indicated in* Fig. 5. The *Gauss* curve attributed to every transition has a bandwidth of 16 nm for the π-π^* transitions and of 14.5 nm for the n-π^* transitions. The peak height is determined from formula (3)

appears at longer wavelength than the $(\pi\text{-}\pi^*)_+$ 'perpendicular' band. In their investigation on finite peptides using the exciton model, *Madison & Schellman* [16] found that the longer-wavelength negative band of the π-π^* system does not develop before the octa- or decamer level is reached. In our own calculations, we notice a gradual redshift of the longest-wavelength π-π^* transition of negative rotatory strength with increasing number of residues (see *Table 5*). It is also of

Table 5. *The π-π^* transition with negative rotatory strength appearing at longest wavelength in the right-handed α-helix.* Computed components of the electric dipole transition moment in au, rotatory strength R and wavelength λ. The z-axis coincides with the helix axis. Notice the relative increase of $\langle\vec{\nabla}\rangle_z$ as the helix grows, as well as the concomitant redshift

Oligomer	$\langle\vec{\nabla}\rangle_x$	$\langle\vec{\nabla}\rangle_y$	$\langle\vec{\nabla}\rangle_z$	$R \cdot 10^{40}$ (cgs)	λ (nm)
Di-	−0.1739	−0.0804	−0.2794	−122	170
Tri-	0.0177	−0.1432	−0.3199	−209	170
Tetra-	0.0580	−0.1438	−0.3106	−190	171
Penta-	−0.2085	−0.0030	−0.4113	−244	177
Hexa-	−0.2353	0.0528	−0.3742	−115	178
Hepta-	0.0071	−0.2188	−0.3967	−188	178
Octa-	−0.1574	0.0606	−0.5147	−381	181
Nona-	−0.1415	0.0003	−0.5396	−499	182

interest that the relative z-component, *i.e.* the 'parallel' component of the electric dipole transition moment of this transition increases. The predicted spectrum of the nonamer is, however, still quite far removed from that encountered in the polymer. The selection rules for the polarization of transitions, valid for the quasi-infinite polymer, only gradually come to play in the growing oligomer. As expected, the n-π^* transitions are also predominantly z-polarized.

In our calculations the energetic splitting of the various π-π^* transitions is somewhat larger, yet comparable to the one resulting from the exciton model [16]. On the other hand, *Madison & Schellman* find that the degeneracy of the n-π^* transitions is scarcely removed in their computations [16], in contrast to our own results. This splitting is of course heavily dependent on the n-π mixing parameter Λ. In Section 3, formula 1c), we have indicated how the local interactions Λ_i couple n and π at the SCF level. In the frame of the single-excitation CI the following nonvanishing nondiagonal matrix elements occur:

$$\text{a)}\ \langle n_i \to \pi_i^* \mid \mathfrak{H} \mid \pi_i \to \pi_i^* \rangle = -\langle \pi_i \pi_i^* \mid n_i \pi_i^* \rangle + 2\langle \pi_i \pi_i^* \mid \pi_i^* n_i \rangle$$

$$\text{b)}\ \langle n_i \to \pi_i^* \mid \mathfrak{H} \mid \pi_j \to \pi_j^* \rangle = 2\langle \pi_j \pi_i^* \mid \pi_j^* n_i \rangle$$

$$\text{c)}\ \langle n_i \to \pi_i^* \mid \mathfrak{H} \mid n_j \to \pi_j^* \rangle = 2\langle n_j \pi_i^* \mid \pi_j^* n_i \rangle$$

$$\text{d)}\ \langle \pi_i \to \pi_i^* \mid \mathfrak{H} \mid \pi_j \to \pi_j^* \rangle = 2\langle \pi_j \pi_i^* \mid \pi_j^* \pi_i \rangle$$

In comparison with the exciton model, these matrix elements may be interpreted in the way indicated below and lead to the following types of contributions to the rotatory strengths:

Type of interaction:	Rotatory strength contribution:
a) local	μ_i-m_i
b) dipole-quadrupole	μ_i-m_j
c) quadrupole-quadrupole	
d) dipole-dipole	μ_i-μ_j

Table 7 shows that the $(n_i \rightarrow \pi_i^*) - (n_j \rightarrow \pi_j^*)$ interaction, while in general significantly smaller than the $(n_i \rightarrow \pi_i^*) - (\pi_j \rightarrow \pi_j^*)$ interaction, is nevertheless non-negligible.

It is also instructive to analyse the excited state wavefunctions. By nature the π-π^* transitions are more delocalized within the molecule than the n-π^* transitions. Several local π-π^* excitations will contribute with comparable weight to a given π-π^* state. On the other hand, a given n-π^* state will mainly contain the $n\pi^*$ configuration of a particular monomer. By separately summing the squares of the CI coefficients of the $n\pi^*$ and $\pi\pi^*$ configurations for a given excited state, one notices that the degree of mixing of these two kinds of configurations is quite extensive (see *Table 6*). This also illustrates the way in which the n-π^* transitions borrow

Table 6. *Results for righthanded α-helical nonaglycine with all $\Delta = 0.5$ eV.* The column labelled '$n\pi^*$' lists the sum of squared CI coefficients for the $n\pi^*$ configurations. The column labelled '$\pi\pi^*$' does the same for the $\pi\pi^*$ configurations. Note the extent of $n\pi^*$-$\pi\pi^*$ mixing. R_{ab} denotes rotatory strengths, f_{ab} oscillator strengths

Excited state b		λ (nm)	$\sum B^2$ $n\pi^*$	$\pi\pi^*$	$R_{ab} \cdot 10^{40}$ (cgs)	f_{ab}
n-π^*	1	245	0.681	0.319	− 12.5	0.006
	2	241	0.661	0.339	− 28.8	0.008
	3	240	0.717	0.283	− 15.0	0.009
	4	238	0.710	0.290	− 46.7	0.015
	5	235	0.697	0.303	− 41.0	0.015
	6	234	0.712	0.288	− 2.56	0.007
	7	232	0.760	0.240	− 39.9	0.017
	8	231	0.773	0.227	− 41.0	0.013
	9	229	0.729	0.271	− 19.8	0.009
π-π^*	10	190	0.360	0.640	90	0.019
	11	189	0.356	0.644	190	0.048
	12	185	0.333	0.667	156	0.059
	13	182	0.290	0.710	−499	0.829
	14	180	0.302	0.698	978	0.412
	15	170	0.245	0.755	−205	0.363
	16	169	0.250	0.750	−142	0.114
	23	164	0.207	0.793	−186	0.034
	24	163	0.215	0.785	− 68	0.027

electric dipole allowedness from the π-π^* transitions. Computed f-values for the transitions in nonaglycine are shown in *Table 6*. In a similar fashion as for the rotatory strengths, we sum the contributions for the composite bands (n-π^*), $(\pi\text{-}\pi^*)_+$ and $(\pi\text{-}\pi^*)_-$ and divide each sum by the number of residues. The connection to the absorption (extinction) coefficient is established by the approximate relation

$$f \approx 4.32 \cdot 10^{-9} \sqrt{\pi}\, \Delta \cdot \varepsilon_{max} \qquad (4)$$

in which Δ is the bandwidth in cm^{-1}. We assume $\Delta(n\text{-}\pi^*)=3000\ cm^{-1}$, $\Delta(\pi\text{-}\pi^*)_+ = \Delta(\pi\text{-}\pi^*)_- = 5000\ cm^{-1}$

$$\begin{aligned} f(n\text{-}\pi^*) &= 0.011 & \varepsilon_{max}(n\text{-}\pi^*) &= 480 \\ f(\pi\text{-}\pi^*)_+ &= 0.060 & \varepsilon_{max}(\pi\text{-}\pi^*)_+ &= 1570 \\ f(\pi\text{-}\pi^*)_- &= 0.152 & \varepsilon_{max}(\pi\text{-}\pi^*)_- &= 3970 \end{aligned}$$

The order of magnitude of these results also seems reasonable (see *Fig. 1*).

Table 7. *CI matrix elements for the nonamer in eV between the configuration* $n_9\pi_9^*$ (here the subscript numbers the amide group on which the MO's are located) *and other configurations* $n_i\pi_i^*$ *and* $\pi_i\pi_i^*$, $i=1,\ldots,9$

	$\langle n_9 \rightarrow \pi_9^* \vert \hat{\mathcal{H}} \vert \ldots \rangle$		
$\vert \pi_9 \rightarrow \pi_9^* \rangle$	0.7584		
$\vert \pi_8 \rightarrow \pi_8^* \rangle$	0.0559	$\vert n_8 \rightarrow \pi_8^* \rangle$	−0.0148
$\vert \pi_7 \rightarrow \pi_7^* \rangle$	−0.0411	$\vert n_7 \rightarrow \pi_7^* \rangle$	0.0167
$\vert \pi_6 \rightarrow \pi_6^* \rangle$	−0.0487	$\vert n_6 \rightarrow \pi_6^* \rangle$	0.0140
$\vert \pi_5 \rightarrow \pi_5^* \rangle$	0.0007	$\vert n_5 \rightarrow \pi_5^* \rangle$	−0.0017
$\vert \pi_4 \rightarrow \pi_4^* \rangle$	−0.0062	$\vert n_4 \rightarrow \pi_4^* \rangle$	0.0018
$\vert \pi_3 \rightarrow \pi_3^* \rangle$	−0.0074	$\vert n_3 \rightarrow \pi_3^* \rangle$	0.0024
$\vert \pi_2 \rightarrow \pi_2^* \rangle$	−0.0019	$\vert n_2 \rightarrow \pi_2^* \rangle$	0.0004
$\vert \pi_1 \rightarrow \pi_1^* \rangle$	−0.0010	$\vert n_1 \rightarrow \pi_1^* \rangle$	0.0002

6. Conclusions. – The aim of this investigation is to find a tractable semi-empirical molecular orbital procedure capable of representing the dominant long-wavelength spectroscopic features of oligopeptides and giving a unified description of both π-π^* and n-π^* transitions. The α-helical oligomers considered in this first paper are rather idealized systems, not directly accessible to experiment. The computed results must therefore be compared with a) experimental data on polypeptides and b) data calculated by the exciton model. Within these restrictions, it appears that the order of magnitude of the electronic properties predicted here is consistent and satisfactory. This warrants applying the procedure to other small peptides. In particular, it is hoped that the method will contribute to the understanding of the (n-π^*)−(π-π^*) interaction and to the interpretation of the influence of long-wavelength absorbing side-chains.

This research was financially supported by the *Swiss National Science Foundation* (Project No. 2.443.0.75). We are also grateful to the *Computer Center* of the University of Zurich for computer time.

REFERENCES

[1] *W. Moffitt*, J. chem. Physics *25*, 467 (1956).
[2] *D. D. Fitts & J. G. Kirkwood*, Proc. Natl. Acad. Sci. USA *42*, 33 (1956).
[3] *W. Moffitt, D. D. Fitts & J. G. Kirkwood*, Proc. Natl. Acad. Sci. USA *43*, 723 (1957).
[4] *F. M. Loxsom*, J. chem. Physics *51*, 4899 (1969).
[5] *C. W. Deutsche*, J. chem. Physics *52*, 3703 (1970); *M. R. Philpott*, J. chem. Physics *56*, 683 (1972).
[6] *A. E. Hansen & J. Avery*, Chem. Physics Letters *13*, 396 (1972).

[7] *W. Moffitt & J. T. Yang*, Proc. Natl. Acad. Sci. USA *42*, 596 (1956).
[8] *N. S. Simmons & E. R. Blout*, Biophys. J. *1*, 55 (1960).
[9] *N. S. Simmons, C. Cohen, A. G. Szent-Gyorgyi, D. B. Wetlaufer & E. R. Blout*, J. Amer. chem. Soc. *83*, 4766 (1961).
[10] *S. Beychok & E. R. Blout*, J. mol. Biol. *3*, 769 (1961).
[11] *G. Holzwarth, W. B. Gratzer & P. Doty*, J. Amer. chem. Soc. *84*, 3194 (1962).
[12] *G. Holzwarth & P. Doty*, J. Amer. chem. Soc. *87*, 218 (1965).
[13] *J. A. Schellman & P. Oriel*, J. chem. Physics *37*, 2114 (1962).
[14] *I. Tinoco, Jr.*, Advan. chem. Physics *4*, 113 (1962); *R. W. Woody & I. Tinoco*, J. chem. Physics *46*, 4927 (1967).
[15] *R. W. Woody*, J. chem. Physics *49*, 4797 (1968).
[16] *V. Madison & J. Schellman*, Biopolymers *11*, 1041 (1972).
[17] *G. Wagnière & R. Geiger*, Helv. *56*, 2706 (1973).
[18] *S. Kawanishi & S. Sano*, Biochemistry *12*, 3166 (1973).
[19] *W. Gans*, Diplomarbeit, University of Zurich 1973.
[20] *R. Hoffmann*, J. chem. Physics *39*, 1397 (1963); *W. Hug & G. Wagnière*, Tetrahedron *25*, 631 (1969).
[21] *J. A. Pople, D. P. Santry & G. A. Segal*, J. chem. Physics *43*, S129 (1965); *J. A. Pople & G. A. Segal*, J. chem. Physics *44*, 3289 (1966).
[22] *R. E. Geiger & G. H. Wagnière*, Helv. *58*, 738 (1975).
[23] Orbital plot program by *E. Haselbach & A. Schmelzer*, Helv. *54*, 1299 (1971).
[24] *R. E. Geiger*, Doctoral dissertation, University of Zurich 1974.
[25] *W. Johnson, jr., & I. Tinoco, jr.*, J. Amer. chem. Soc. *94*, 4389 (1972).
[26] *R. Pariser & R. G. Parr*, J: chem. Physics *21*, 466, 767 (1953); *J. A. Pople*, Proc. phys. Soc. A*68*, 81 (1955).
[27] *R. G. Parr*, 'The Quantum Theory of Molecular Electronic Structure', Benjamin Inc., New York 1963, Chap. 13; *G. Wagnière*, 'Introduction to Elementary Molecular Orbital Theory and to Semiempirical Methods', Springer Verlag, Heidelberg 1976, Chap. IV, V, and references cited therein.
[28] *D. W. Turner, C. Baker, A. D. Baker & C. R. Brundle*, 'Molecular Photoelectron Spectroscopy', Wiley Interscience, London 1970, p. 132–138.
[29] *J. N. Murrell*, 'The Theory of Electronic Spectra of Organic Molecules', Methuen & Co., London 1963, Chap. 8.
[30] *M. B. Robin*, 'Higher Excited States of Polyatomic Molecules', Vol. II, Academic Press, New York 1975, p. 75–106, p. 121–160.
[31] *H. Labhart & G. Wagnière*, Helv. *46*, 1314 (1963).
[32] *G. Blauer & G. Wagnière*, J. Amer. chem. Soc. *97*, 1949 (1975).
[33] *G. Wagnière & G. Blauer*, J. Amer. chem. Soc. *98*, 7806 (1976).
[34] *W. Hug & G. Wagnière*, Theoret. chim. Acta *18*, 57 (1970).